




# Particle shape characterization of shaking table streams in a Turkish chromite concentration plant by using dynamic imaging and microscopical techniques

Ugur Ulusoy & Osman Nuri Atagun


To cite this article: Ugur Ulusoy & Osman Nuri Atagun (2023) Particle shape characterization of shaking table streams in a Turkish chromite concentration plant by using dynamic imaging and microscopical techniques, Particulate Science and Technology, 41:2, 141-150, DOI: [10.1080/02726351.2022.2046666](https://doi.org/10.1080/02726351.2022.2046666)


To link to this article: <https://doi.org/10.1080/02726351.2022.2046666>

 View supplementary material 

 Published online: 07 Mar 2022.

 Submit your article to this journal 



 Article views: 196

 View related articles 

 View Crossmark data 



# Particle shape characterization of shaking table streams in a Turkish chromite concentration plant by using dynamic imaging and microscopical techniques

Ugur Ulusoy<sup>a,b</sup>  and Osman Nuri Atagun<sup>a</sup> 

<sup>a</sup>Mining Engineering Department, Sivas Cumhuriyet University, Sivas, Turkey; <sup>b</sup>Chemical Engineering Department, Sivas Cumhuriyet University, Sivas, Turkey

## ABSTRACT

To the best of the authors' knowledge, this study is one of its kind since it is related to the quantitative shape examination of particles of feed, concentrate, middling and tailing products in coarse and fine shaking table streams of a Turkish chromite concentration plant. In this study, the novel technique; Dynamic image analysis (DIA) as well as visual inspection by SEM and stereomicroscope were used for the representative samples of the plant. Analysis revealed that particle shapes of concentrate products are mostly equant or round while the most elongated particles were observed in tailing products at a 95% confidence level. This is highly linked to the rolling and sliding movement of round and elongated particles, respectively on the deck. This implies that particle shape is one of the parameters affecting gravity separation. Using shape data with tonnages of the circuits in mass balance equations indicates that shape distributions of products in table circuits are consistent. This study gives insight as better separation recovery could be obtained when a proper mill is used for producing feed particles, which have targeted shape to shaking tables since any improvements in recovery will have a big effect on the concentrate income.

## KEYWORDS

Chromite; particle shape; dynamic image analysis; aspect ratio; shaking table

## 1. Introduction

Chromium, which has unique resisting power to high corrosion and high temperature, is of considerable importance for chemical, refractory, and metallurgical industries (Guertin, Jacobs, and Avakian 2005) and is regarded as significant raw material for low-carbon technologies and energy production. Therefore, it is considered as a critical mineral (economically important and subject to high risks of supply) according to the US Department of Interior (Fortier et al. 2018) and Geoscience Australia in 2018 (Mudd et al. 2018), although it is near to the level of supply risk for Europe in 2020 (European Commission 2020).

Recently, gravity separation is regaining popularity as it creates relatively less environmental pollution (Brits 1991). Since high-grade chromite ores have been diminishing day by day due to the increasing global demand, beneficiation of low-grade chromite ores by gravity separators like spirals and shaking table is a widely accepted way of concentration due to its cheapness and environmental friendliness (Murthy, Tripathy, and Kumar, 2011).

Although various attempts were conducted on optimizing the effect of operating variables on the performance of gravity separation for heavy mineral recovery, in the recent decade the experimental works using methods of physical separation have shown the worth of particle geometry, such

as particle size and shape (Güven and Çelik 2016; Pita and Castilho 2016; Pita and Castilho 2017; Richard et al. 2017; Phengsaart et al. 2018). Although shaking table mainly separates particles based on their densities, to some degree, it also separates particles by their sizes and shapes (Richards and Locke 1940; Sivamohan 1985; Brits 1991; Aplan 2003; Das 2009; Singh et al. 2014). Since separation depends to a large degree on the hydraulic displacement of the particles, their shape influences their movements (Pryor 1965), i.e., flat particles have less tendency to roll and complicate the separation. Moreover, the velocities of the moving particles with a different shape in the water medium will be different as they are subjected to different resistance forces in the medium (Ofori-Sarpong and Amankwah 2011). For example, mica could be separated from feldspar, owing to its laminar shape by using shaking table at  $-0.212 + 0.074$  mm size (Kademli and Gulsoy 2012). Another interesting example is that the lamellar shape vanadium-bearing particle would be protected in the grinding process and the operation parameters and table deck structure would be optimized according to the shape factor to improve the separation effect (Zhao et al. 2013).

The influence of different grinding systems has been receiving more attention due to their significant role on the shape of particles. It has been reported that desired mineral product shape can be obtained by using a proper mill since

the particle shape of minerals is generally ruled by grinding (except for mica due to its structure and cleavage). For instance, the highest elongated quartz particles were found in rod mill products compared to the ball and autogenous mill (Hicyilmaz et al., 2006), whilst the higher elongated magnetite particles were obtained by ball mill compared to rod mill (Dehghani, Rahimi, and Rezai 2012). On the other hand, the higher elongated platinum group mineral particles were found in the ball mill compared to stirred mill (Little et al. 2017). Besides, different shapes of the gold particle can be produced by using different mills, such as disk mill, ball mill, vibratory pulverizer, and hammer mill to achieve higher enrichment ratios and higher recovery in separation with Knelson concentrator (Ofori-Sarpong and Amankwah 2011).

Actually, the hypothetical improvement of gravity beneficiation has not yet arrived at the phase at which the particle attributes essential for the best efficiency of a shaking table can be forecasted (Sivamohan 1985). Since the recovery of gravity separation is generally lower than others, a small increase in separation recovery will mean a large contribution to concentrate income (Wills and Finch 2015; Fitzpatrick et al. 2016). Therefore, particle characteristics need to be measured for the understanding of separation performance (Grobler and Bosman 2011) for ensuring operation at best conditions and optimizing separation efficiency. Although there are many works interested in various ore beneficiation using the shaking table on laboratory and pilot scale, examination of particle shape of shaking table products of an industrial concentration plant by dynamic image analysis (DIA) is still lacking. Therefore, the purpose of this study is 4-fold:

1. to quantify particle shape of all products in the shaking table circuits of a Turkish chromite beneficiation plant by DIA in terms of different aspect ratio (AR) parameters as well as visual techniques, namely scanning electron microscope (SEM) and stereo-microscopy,
2. to prove the significance of the mean AR values of each stream by analysis of variance (ANOVA) whether they are the same or different.
3. to reveal what kind of particles (round or elongated) are dominant in the concentrate and tailing products,
4. to understand how these particles behave on the flowing film concentration by shaking table. Thus, a proper mill could be used to generate suitable grain-shaped feed material to achieve a better table separation performance.

## 2. Materials and method

### 2.1. Sample preparation

Representative samples were taken from the Turkish plant (Aksu Group Mining Industry Co. Inc. at Kangal district of Sivas in Turkey) treating low-grade chromite ores by gravity separation method using spirals and shaking tables.

In the plant, run-of-mine chromite ore is first ground by a ball mill from 15 mm down to 2 mm. Then, stack-sizer ( $-0.400$  mm) and hydrocyclone ( $-0.400 + 0.075$  mm) were used for classification purposes before spiral circuits (rougher and scavenger) as a pre-concentration stage. Finally, HMT sizer (crossflow) and hydrosizer classifications were used to prepare the feed streams of the coarse ( $-0.425 + 0.212$  mm) and fine ( $-0.212 + 0.075$  mm) size shaking tables.

It should be emphasized that this study is only focused on shape quantification of shaking table circuits, since the particle size limit of DIA is  $-0.250$  mm, and the particle size range of the fine shaking table operating in the plant is  $-0.212 + 0.075$  mm. Table 1 summarizes the operating conditions of shaking tables.

Chromite ore fed into the shaking tables contains not only valuable minerals namely chromite but also gangue minerals, such as forsterite and brucite. Other minor minerals in the gangue are mostly quartz and calcite. The density of chromite, forsterite, brucite, calcite, and quartz minerals are 4.80, 3.27, 2.40, 2.65, and 2.65  $\text{gr}\cdot\text{cm}^{-3}$ , respectively. Other physical properties of the minerals to be separated were given in Table 2.

Representative samples for feed, concentrate, middling and tailing products of coarse and fine size shaking tables were taken by using a specially designed sampler cutter, which has a rectangular cross-section (Figure 1(a)) from the sampling points of circuits as shown in Figure 1(b). Each sample was stored in sealed bags and labeled. Afterward, it was spread on an aluminum tray and dried using a propane stove. Finally, the sample amounts were reduced by the cone and quartering technique.

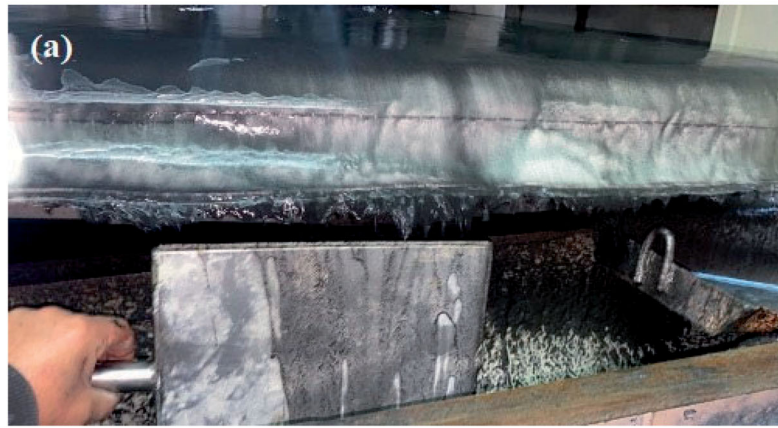
To eliminate the effect of particle size on the shape characterization, samples belonging to feed, concentrate, middling and tailing products of coarse and fine size tables were sieved to prepare two narrow-size fractions ( $-0.180 + 0.125$  mm and  $-0.125 + 0.090$  mm) for the shape characterization tests. Sieving operation was performed by using Retch laboratory standard sieves along with Endecotts sieve shaker (Octagon 200, Endecotts Ltd, UK) at  $6 \times 10^2$  s with a 40 amplitude and continuous frequency.

**Table 1.** Operating conditions of shaking tables operated in the chromite beneficiation plant.

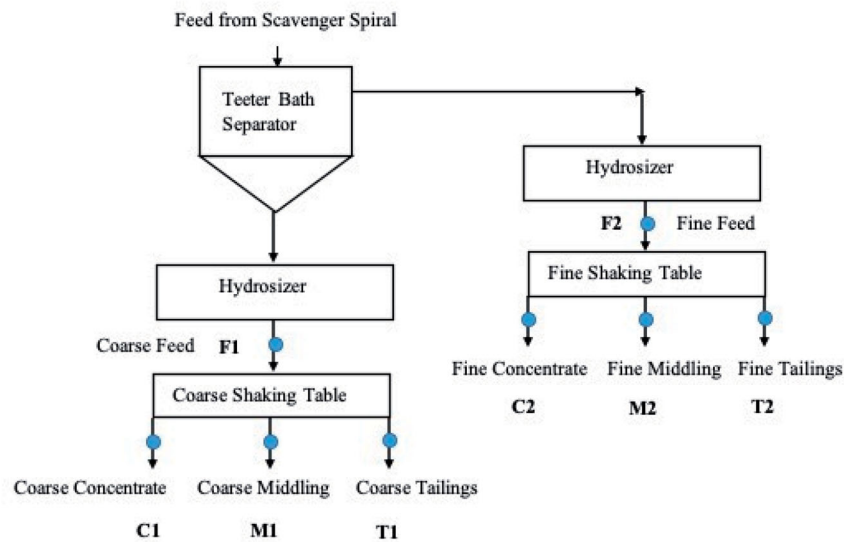
Operating parameters	Coarse table	Fine table
Type	Wilfley	Wilfley
Length $\times$ width $\times$ height (m)	L6.800 $\times$ W2.400 $\times$ H3.200	L6.800 $\times$ W2.400 $\times$ H3.200
Deck area ( $\text{m}^2$ )	8	8
Particle size (mm)	$-0.425 + 0.212$	$-0.212 + 0.075$
Stroke (m)	$1.5 \times 10^{-2}$ – $2.0 \times 10^{-2}$	$1.0 \times 10^{-2}$ – $1.5 \times 10^{-2}$
Wash flow rate ( $\text{m}^3\text{s}^{-1}$ )	$4.1 \times 10^{-4}$ – $5.5 \times 10^{-4}$	$4.1 \times 10^{-4}$ – $5.5 \times 10^{-4}$
Feed rate ( $\text{kg}\text{s}^{-1}$ )	0.194–0.25	0.125–0.194
Tilt angle ( $^\circ$ )	3	3
Deck speed ( $\text{r}\text{m}^{-1}$ )	290–310	300

**Table 2.** Physical properties of the minerals in the run-of-mine chromite ore.

Mineral	Chromite	Forsterite	Brucite	Calcite	Quartz
Formula	FeO·Cr <sub>2</sub> O <sub>3</sub>	Mg <sub>2</sub> (SiO <sub>4</sub> )	Mg(OH) <sub>2</sub>	CaCO <sub>3</sub>	SiO <sub>2</sub>
Weight distr. %	5.249	86.464	5.477	1.239	0.205
Color	Black	Green, yellow, white	White, yellow, grayish	White, yellow, grayish	White, yellow, grayish
Appearance	Metallic	Transparent	Transparent	Transparent to opaque	Transparent to opaque
Crystal system	Isometric	Orthorhombic	Trigonal-hexagonal	Hexagonal	Hexagonal
Specific gravity	4.80	3.27	2.40	2.65	2.65



(b)

**Figure 1.** (a) Sample cutter, (b) Sampling points of coarse and fine shaking table circuits in the chromite beneficiation plant.

A few grams of the representative samples reduced by micro rotary riffler were placed in a  $2.5 \times 10^{-5}$  L glass beaker with distilled water and held in the ultrasonic bath at  $1.8 \times 10^2$  s to obtain well-dispersed particles for dynamic imaging.

## 2.2. Determination of AR parameters of particles by DIA

In this study, the shapes of particles were quantified with three AR parameters based on different shape models used in DIA. That is, the Bounding rectangle aspect ratio (BRAR), elliptical aspect ratio (EAR), and Feret aspect ratio (FAR) are based on the rectangle, ellipse, and irregular model (Ulusoy 2020), respectively. While EAR is formularized as the ratio of length to width of equivalent elliptical

area based on the ellipse model (Figure 2(a)), BRAR is defined as the ratio of the larger side to the smaller side of the bounding rectangle is given by Figure 2(b). Similarly, FAR is described by the ratio of Feret length to Feret width (Figure 2(c)) based on an irregular model (Vision Analytical 2021). Figure 2 illustrates how AR values change with the shape of the particles. It should be noted that AR values are equal to 1.0 for spherical particles, whereas it takes the highest value for needlelike particles.

Particle shape characterization was performed by using the DIA instrument (Particle Insight, Micromeritics® Instrument Corp., Norcross, GA, USA) (Vision Analytical, 2021). The working principle of DIA is based on the capturing of particle images while they are flowing on a dynamic turbulent flow route in front of the digital camera (see Figure 2(d)). It has unique properties like random orientation and

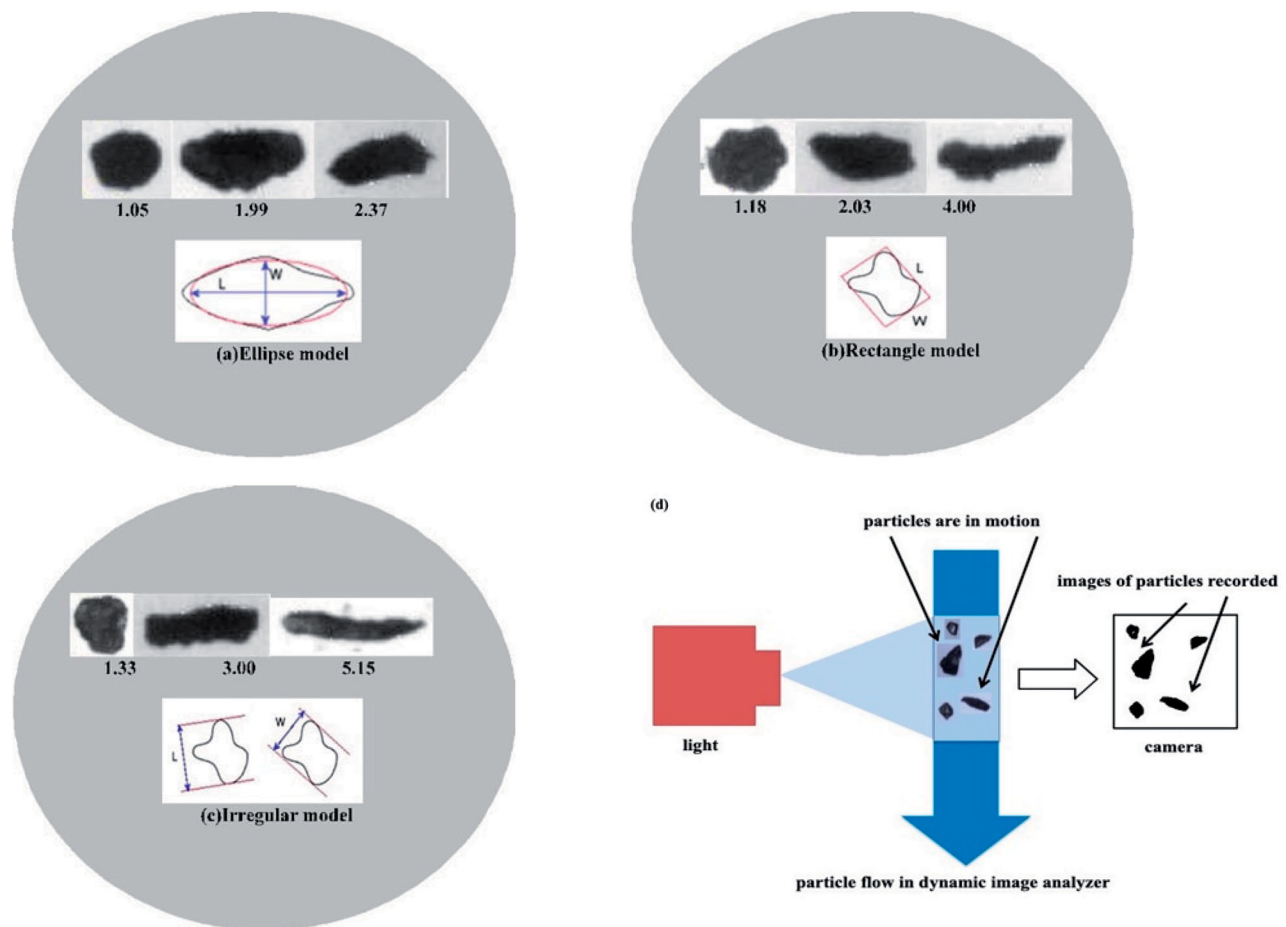


**Figure 2.** Particle shape model used in DIA and extreme values of AR as a function of particle shape for (a) ellipse model (b) rectangle model, (c) irregular model (Vision Analytical 2021), (d) imaging process mechanism used by DIA.

recirculation for the analysis of particles from all angles for the best and most accurate representation.

More than  $10^4$  particles were measured for each sample to obtain high statistical accuracy since it has been reported that more than  $6.4 \times 10^3$  particles per image measurement are required at 99% confidence level (Allen 1990; BS 3406-4 1993). Measurements were repeated at least three times and the mean values of three consistent measurements were used for the shape characterization tests.

### 2.3. SEM analysis

The shape features of the same representative samples used for DIA were also characterized by SEM (Tescan MIRA3 XMU model, Czech Republic) at 20 kV. Powder samples were sprinkled onto a carbon tape before SEM examination.

### 2.4. Stereo-microscopical analysis

Visual inspection of particle shapes of the same representative samples used in DIA was also performed by using a stereo-microscope (BOECO, BOECO Binocular Microscope BM-180/1-AC model, Germany) ( $\times 40$ ).

## 3. Results and discussion

### 3.1. DIA results

Figure 3 presents comparative AR values (BRAR, EAR, and FAR) of each product (feed, concentrate, middling, and tailing) of coarse and fine size tables at both size fractions. As clearly seen from Figure 3, there is a common trend of  $AR_{Conc.} < AR_{Midd.} < AR_{Feed} < AR_{Tail.}$  for all tested AR parameters. This implies that there are shape differences at the same size fraction for feed, concentrate, middling and tailing products of coarse and fine size shaking tables. It was found that all the concentrate products have the lowest AR values, while all the tailing products have the highest AR values. Considering coarse size shaking tables (Figures 3(a,c,e)), AR values of coarse size fractions ( $-0.180 + 0.125$  mm) are lower than those of fine size fractions ( $-0.125 + 0.090$  mm). Interestingly, the differences between the AR values of coarse and fine size fractions appear to be quite large (Figures 3(a,c,e)). On the other hand, this difference is comparatively small for fine size tables (see Figures 3(b,d,f)). As seen from Figures 3(b,d,f), AR values of fine size fractions ( $-0.125 + 0.090$  mm) had generally lower than those of coarse ( $-0.180 + 0.125$  mm) size fractions (except for concentrate products for BRAR, EAR, and FAR values, and middling product for FAR values). But, when AR values of only concentrate products are

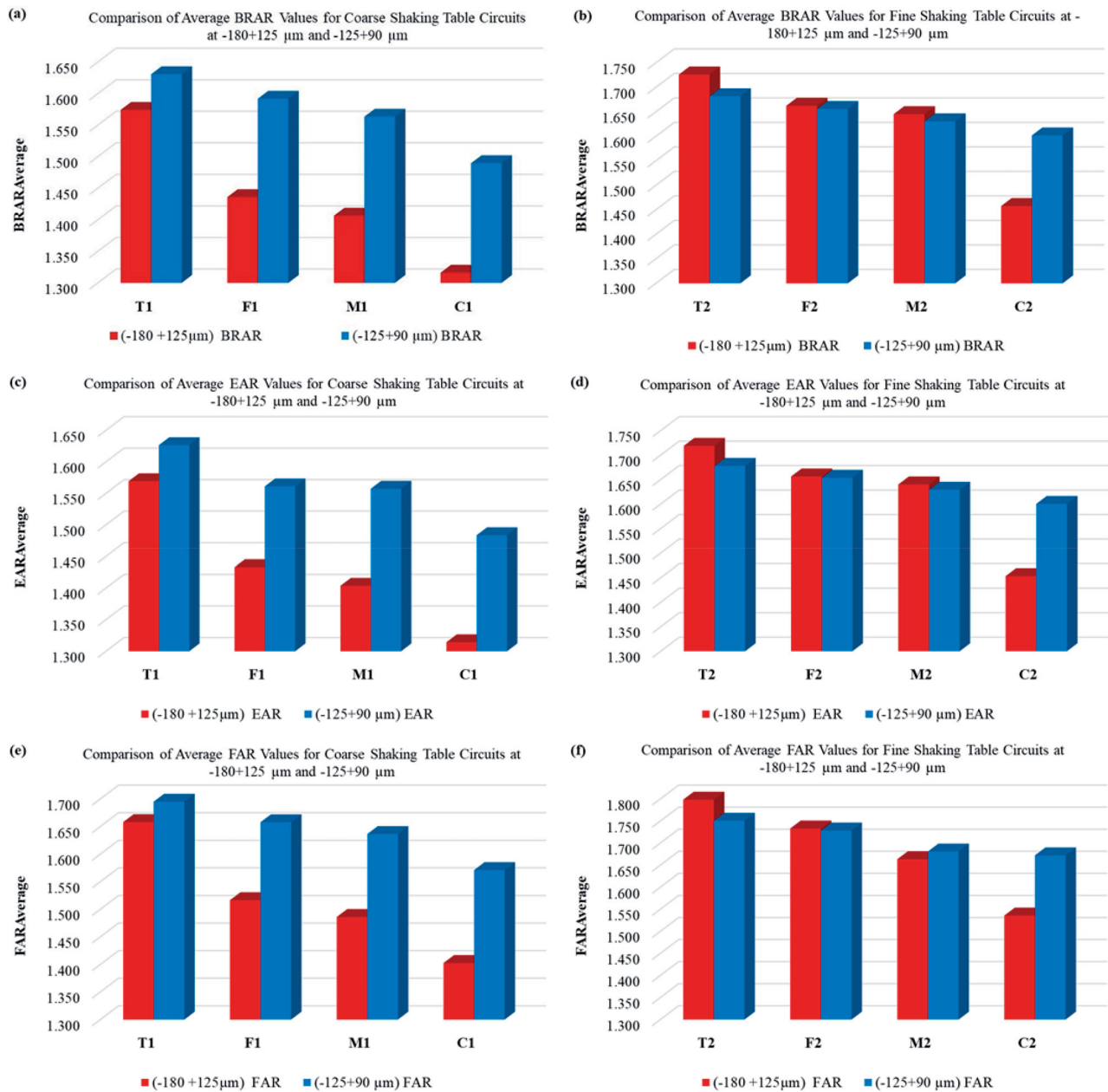


**Figure 3.** Effect of particle size fractions on the average AR parameters of coarse and fine shaking table, (a)  $BRAR_{Average}$  values for coarse shaking table circuit, (b)  $BRAR_{Average}$  values for fine shaking table circuit, (c)  $EAR_{Average}$  values for coarse shaking table circuit, (d)  $EAR_{Average}$  values for fine shaking table circuit, (e)  $FAR_{Average}$  values for coarse shaking table circuit, (f)  $FAR_{Average}$  values for fine shaking table circuit.

compared with tailing products for both tables and size fractions (Figure 3), it can be deduced that concentrate products have the most-round particles, whereas, tailing products have the most elongated particles. Figure 4, which was given as an example for illustrating the thumbnail images of the particles in concentrate and tailing products of coarse size table at coarse size ( $-0.180+0.125\ \text{mm}$ ) fractions, also supports this result. Although not all the particles are in the same shape, the concentrate product contains dominantly blocky, equant, or regular particles, on the other hand, rod-like or elongated particles are mostly observed in the tailing product. This indicates that particle shape can be an effective criterion for the separation of differently shaped particles, such as regular and elongated. Results are in good agreement with the previously reported studies (Thompson

1958; Napier-Munn and Alford 1991; Kademli and Gulsoy 2012; Zhao et al. 2013; Pita and Castilho 2016; Boucher 2017).

### 3.2. Statistical evaluation of the DIA results

One-way ANOVA (Ulusoy 2018) was employed to determine whether the mean AR parameters of table products were statistically different from each other using IBM<sup>®</sup> SPSS<sup>®</sup> Statistics version 23 at the confidence level of 95%. All ANOVA Results were summarized in 9 tables, which were given as were [Supplementary Materials](#). Table 3 can be given as an example for the statistical evaluation of the DIA results. Since the “Sig.” value, which is 0.00 (framed in red) is less than the alpha value of 0.05, the  $H_0$  hypothesis was

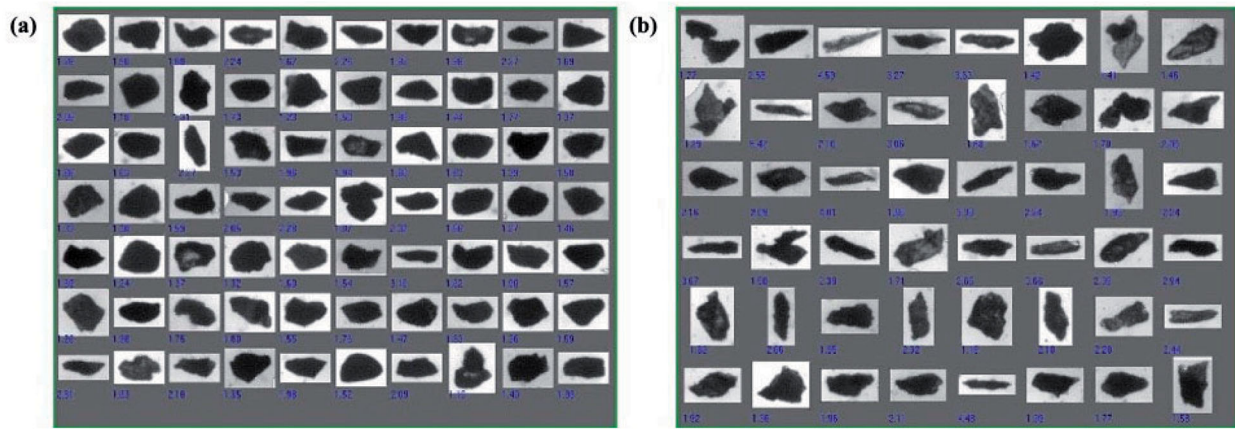


**Figure 4.** Comparison of DIA images of particles in the products of (a) concentrate and (b) tailing for coarse shaking table at coarse size ( $-0.180 + 0.125$  mm) fractions.

**Table 3.** ANOVA test summary for mean BRAR values of coarse shaking table circuit for  $-0.180 + 0.125$  mm size fraction at  $\alpha = 0.05$  (1st measurement).

Descriptives	N	Mean	Std. Dev.	Std. Error	95% Conf. Inter. For Mean	
					Lower bound	Upper bound
F1	10,160	1.53992	.410024	.004068	1.53195	1.54790
C1	10,283	1.47057	.446267	.004401	1.46194	1.47920
M1	10,051	1.48462	.394596	.003936	1.47690	1.49233
T1	10,014	1.61997	.474943	.004746	1.61067	1.62928
Total	40,508	1.52838	.436506	.002169	1.52413	1.53264
Test of homogeneity of variances			Levene Statistic	df1	df2	Sig.*
Based on mean			93.136	3	40,504	.000
ANOVA BRAR		Sum of squares	df	Mean square	F	Sig.**
Between groups		138.982	3	46.327	247.580	.000
Within groups		7579.116	40,504	.187		
Total		7718.098	40,507			

\*Test for homogeneity of variances is significant.

\*\*p-Value indicating significant difference between groups.

rejected. This implies that mean BRAR values of feed, concentrate, middling and tailing products in the table circuit are not equal. The results can be reported as  $F_{(3, 40504)} = 247.580$ ,  $p = 0.00$ . Similar results were found for all measurements of BRAR as well as for EAR and FAR average values measured for all the collected samples (see [Supplementary Materials](#) for other tables).

### 3.3. SEM results

When the same samples used in DIA were characterized by SEM tests, the shape differences between concentrate and tailing particles can be clearly seen in [Figure 5](#). SEM images have shown that concentrate particles are mostly round, whilst the tailing product contains mostly elongated particles.

### 3.4. Stereo-microscope results

Stereo-microscopical images not only help to see the color differences of particles in the samples but also give insight for characterization the shape of the valuable and gangue minerals in the various products as well as liberated particles. As seen from [Figure 6](#), all particles are sufficiently liberated for the gravity concentration (more than 80% for separation processes). Since concentrate grade (46–48%

$\text{Cr}_2\text{O}_3$ ) is higher than tailing, concentrate products ([Figure 6\(a\)](#)) have more chromite particles (black colored), but tailing products have some small chromite particles although they contain highly gangue minerals (light-colored) like forsterite brucite and quartz. Moreover, tailing particles are mostly elongated, while concentrate particles are mostly round. As seen from [Figure 6\(b\)](#) tailing products contains a minor amount of chromite particles. The shapes of these particles are also elongated as well as gangue particles. This implies that particle shape played a role as well as density and size on the separation.

### 3.5. Evaluation of movement of particles having different shapes on shaking table

Since shaking table separation depends to a large degree on the hydraulic displacement of the particles, their shape influences their movements. Based on the DIA results, [Figure 7\(a\)](#) schematically illustrates the shape distribution of particles on shaking tables. As clearly seen from [Figure 7\(a\)](#) feed, concentrate, middling and tailing products have different average AR values, i.e., the most round or equant chromite particles were collected in concentrate product, whereas the most elongated or rod-like gangue particles were accumulated in tailing product. This

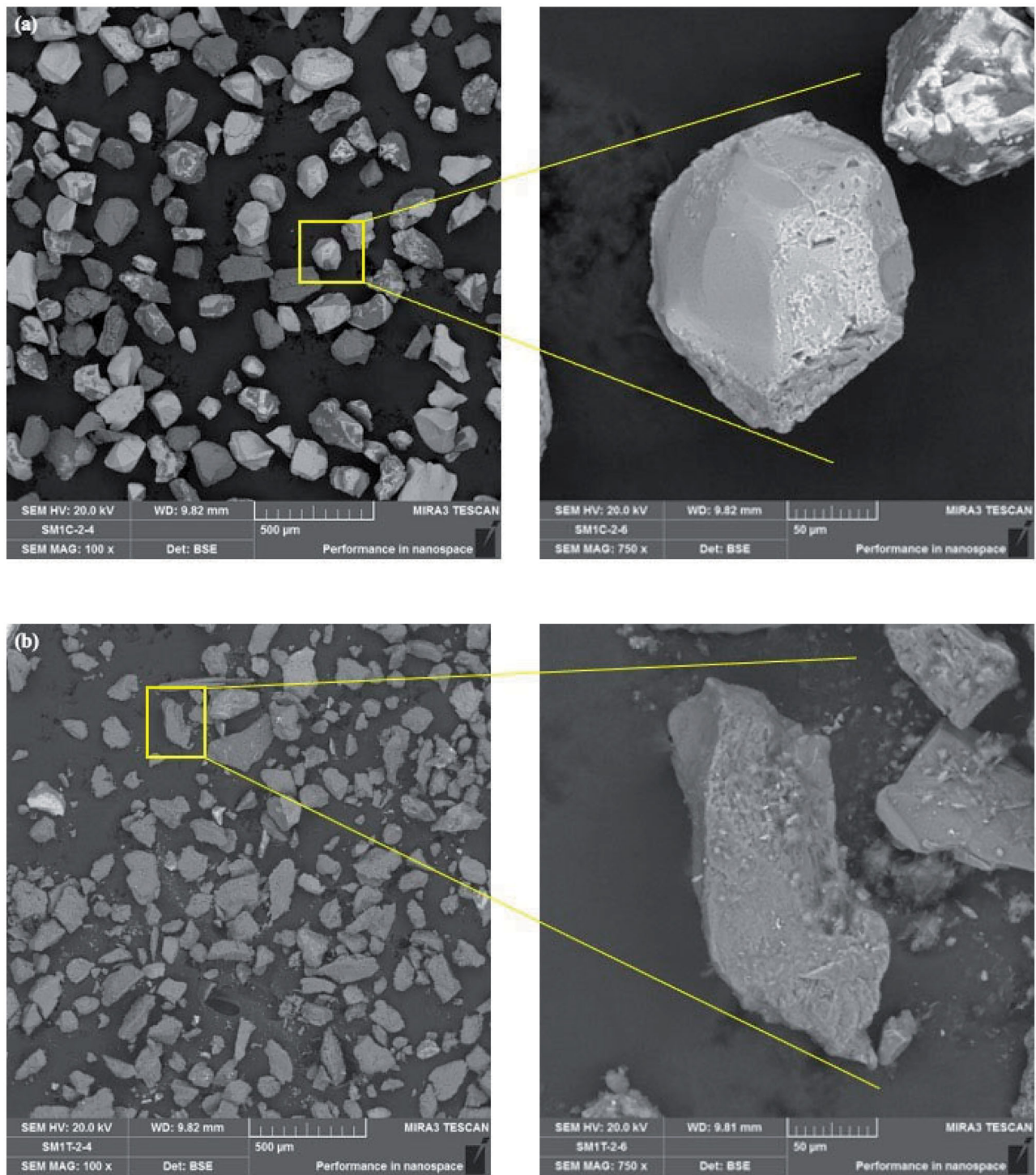


**Figure 5.** Comparison of SEM images of particles (in group and single magnified) in the (a) concentrate and (b) tailing products for coarse shaking table at coarse sized fraction ( $\times 100$ ) and ( $\times 750$ ).

indicates that not only density and size but also the shape of particles affect the separation (Walsh and Kelly 1992; Das 2009). Because particles with different shapes are subjected to different drag forces in the water medium. This causes different movements of particles in the water medium in shaking table separation (Ofori-Sarpong and Amankwah 2011).

When the mixture of particles having near sizes but different densities and shapes are fed to the upper right-hand corner of the deck, the round and heavy chromite (black

colored) particles tend to sit at the bottom of the riffle and roll with the flowing film to the concentrate launder, on the other hand, elongated and light gangue mineral particles (light-colored) tend to slide toward the tailing launder of the shaking table as shown in Figure 7(b).

### 3.6. Mass balance regarding AR values

Although grade and tonnage values are generally used for mass balancing of any concentration unit, any assay values



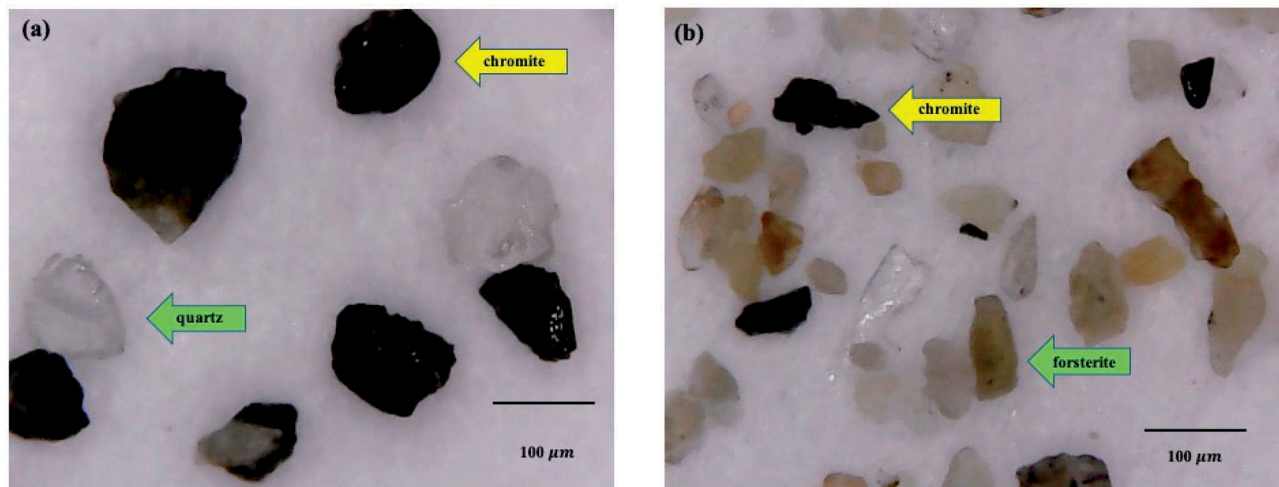


**Figure 6.** Comparison of stereo-microscopical images belongs to (a) concentrate and (b) tailing products for fine shaking table at  $-0.180 + 0.125$  mm sized fraction ( $\times 40$ ).

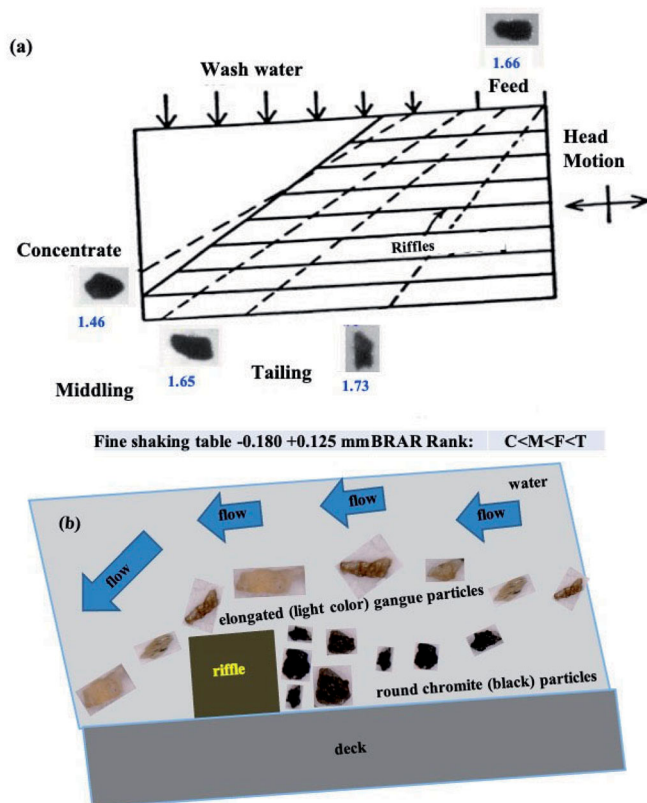


**Figure 7.** (a) Shape distribution on the fine shaking table at coarse size fraction ( $-0.180 + 0.125$  mm), (b) Movement of the particles according to their shape on a shaking table concentration.

like grade, the ratio of water/solid, particle size and solids percentage (Wills and Finch 2015), density, shape, hydrophobicity, adhesion ability, magnetic and electric characteristics (Drzymala 2007) can also be used. So, shape data in terms of mean AR values (BRAR, EAR, and FAR) for feed, concentrate, middling and tailing products of the coarse and fine size shaking tables were utilized in the mass balance equation ( $F_f = C_c + M_m + T_t$ ) to verify the shape distributions of the table products in the circuit. Here, F, C, M, and T denote tonnages of feed, concentrate, middling, and

**Table 4.** Assay and tonnage values of coarse and fine shaking table for mass balance calculations.

Shaking table	Sample name	Grade (%Cr <sub>2</sub> O <sub>3</sub> )	Tonnage (t/h)
Coarse	F1	12.48	2.220
	C1	48.00	0.423
	M1	21.50	0.125
	T1	2.82	1.672
Fine	F2	6.7	3.330
	C2	48.00	0.206
	M2	22.63	0.317
	T2	1.87	2.807

tailing, respectively. On the other hand, f, c, m, and t represent AR values of feed, concentrate, middling, and tailing, respectively.

When mean AR values were used instead of grade along with the tonnage values of each stream (Table 4) in the mass balance equation, it was found that both sides of the equations were balanced. This implies that DIA data are significant and shape distributions of shaking table streams are consistent.

#### 4. Conclusions and future recommendations

The shapes of particles from all streams of the shaking table concentration circuits in the Turkish chromite concentration plant were quantitatively characterized by DIA. Besides, ANOVA tests have shown that mean AR values of feed, concentrate, middling and tailing products for each stream are different at a 95% confidence level.

DIA analysis revealed that AR values of particles in the concentrate products were the lowest indicating that the most round, bulky, or equi-dimensional particles were observed at the concentrate product. On the other hand, the most elongated particles were found in the tailing product of the coarse and fine size tables for both size fractions. DIA results were also supported by visual inspection using SEM and stereo-microscope. The remarkable shape differences between the concentrate and tailing products of the shaking tables were attributed to their different movement in the

flowing film (i.e., round particles tend to roll while elongated particles tend to slide on the deck).

To verify the shape distributions of products in the shaking table circuits, mean AR values were used in the mass balance equations with tonnage, it was found that they are consistent.

This study has shown that particle geometry including particle size and shape as well as density of the minerals play a crucial role in the separation by shaking table. Thus, better separation performance could be obtained if a proper milling system is used for producing feed particles, which have the required shape for shaking tables since any increments in separation recovery mean a big effect on concentrate income.

## Nomenclature

AR	aspect ratio
ANOVA	analysis of variance
BRAR	bounding rectangular aspect ratio
EAR	elliptical aspect ratio
FAR	Feret aspect ratio
DIA	dynamic Image Analysis
SEM	scanning electron microscope

## Acknowledgments

Aksu Group Mining Industry Co. Inc. is gratefully acknowledged for making data available, providing a representative sample as well as for kind permission to publish this paper. The authors would also like to thank Professor Zhiyong Gao, who is the editor of the Physicochemical Problems of Mineral Processing, for his help in checking the English grammar and spelling of the revised article.

## Disclosure statement

The authors declare no conflict of interest.

## ORCID

Ugur Ulusoy  <http://orcid.org/0000-0002-2634-7964>

Osman Nuri Atagun  <http://orcid.org/0000-0003-0032-2889>

## References

- Allen, T. 1990. *Particle size measurement*. 4th ed. New York, NY: Chapman & Hall.
- Aplan, F. F. 2003. Chapter 6: Gravity concentration. In *Principles of mineral processing*, ed. M. C. Fuerstenau and N. H. Kenneth, 185–219. Littleton, CO: SME.
- Boucher, D. 2017. Observation of iron ore particle flow in a mineral spiral concentrator by position emission particle tracking (PEPT). PhD diss., McGill University.
- BS 3406-4. 1993. British Standards 3406, Methods for determination of particle size distribution, Part 4: Guide to microscope and image analysis methods.
- Brits, B. R. 1991. Effect of particle size in gravity separation processes at Palabora, South Africa. In *African mining '91*. Dordrecht: Springer. 159–67. doi:10.1007/978-94-011-3656-3\_16.
- Das, A. 2009. Chapter 1, mineral processing. In *A continuing education course for metallurgy for engineers*. December 14–16. JAMshedpur: NML.
- Dehghani, F., M. Rahimi, and B. Rezaei. 2012. Influence of particle shape on the flotation of magnetite, alone and in the presence of quartz particles. *The Journal of the Southern African Institute of Mining and Metallurgy* 113 (12):905–11.
- Drzymala, J. 2007. *Mineral processing, foundations of theory and practice of mineral processing*. 1st ed. Wrocław: Wrocław University of Technology, Oficyna Wydawnicza PWR.
- European Commission. 2020. Study on the EU's list of critical raw materials. *Factsheets on Non-Critical Raw Materials*. 1:1-595. doi:10.2873/587825.
- Fitzpatrick, R. S., Y. Ghorbani, P. Hegarty, and G. Rollinson. 2016. Quantitative mineralogy for improved modelling of shaking tables. IMPC 2016: XXVIII International Mineral Processing Congress Proceedings – ISBN: 978-1-926872-29-2, 11–15 September. Quebec City: Canadian Institute of Mining, Metallurgy and Petroleum.
- Fortier, S. M., N. T. Nassar, G. W. Lederer, J. Brainard, J. Gambogi, and E. A. McCullough. 2018. Draft critical mineral list—Summary of methodology and background information—U.S. Geological Survey technical input document in response to Secretarial Order No. 3359: U.S. Geological Survey Open-File Report 2018–1021, 15 p. doi:10.3133/ofr20181021.https://pubs.usgs.gov/of/2018/1021/ofr20181021.pdf (accessed October 8, 2021).
- Grobler, J. D., and J. B. Bosman. 2011. Gravity separator performance evaluation using Qemscan® particle mineral analysis. *The Southern African Institute of Mining and Metallurgy* 111:401–8.
- Guertin, J., J. A. Jacobs, and C. P. Avakian. 2005. *Chromium (VI) handbook*. 1st ed. Independent Environmental Technical Evaluation Group (IETEG). Boca Raton, FL: CRC Press.
- Güven, O., and M. S. Çelik. 2016. Interplay of particle shape and surface roughness to reach maximum flotation efficiencies depending on collector concentration. *Mineral Processing and Extractive Metallurgy Review* 37 (6):412–7. doi:10.1080/08827508.2016.1218873.
- Hıçılılmaz, C., U. Ulusoy, S. Bilgen, M. Yekeler, and G. Akdoğan. 2006. Response of rough and acute surfaces of pyrite with 3-D approach to the flotation. *Journal of Mining Science* 42 (4):393–402. doi:10.1007/s10913-006-0068-x.
- Kademli, M., and O. Y. Gulsoy. 2012. The role of particle size and solid contents of feed on mica-feldspar separation in gravity concentration. *Physicochemical Problems of Mineral Processing* 48 (2): 645–54. doi:10.5277/ppmp120227.
- Little, L., A. N. Mainza, M. Becker, and J. Wiese. 2017. Fine grinding: How mill type affects particle shape characteristics and mineral liberation. *Minerals Engineering* 111:148–57. doi:10.1016/j.mineng.2017.05.007.
- Mudd, G. M., T. T. Werner, Z.-H. Weng, M. Yellishetty, Y. Yuan, S. R. B. McAlpine, R. G. Skirrow, and K. Czarnota. 2018. *Critical minerals in Australia: A review of opportunities and research needs*. Records 2018/051. Canberra: Geoscience Australia. <https://ecat.ga.gov.au/geonetwork/srv/eng/catalog.search#/metadata/124161> (accessed October 8, 2021).
- Murthy, Y. R., S. K. Tripathy, and C. R. Kumar. 2011. Chrome ore beneficiation challenges & opportunities – A review. *Minerals Engineering* 24 (5):375–80. doi:10.1016/j.mineng.2010.12.001.
- Napier-Munn, T. J., and R. A. Alford. 1991. The causes of heavy mineral loss from mineral sands wet concentrators. *The AusIMM Proceedings* 296 (1):19–30.
- Ofori-Sarpong, G., and R. K. Amankwah. 2011. Comminution environment and gold particle morphology: Effects on gravity concentration. *Minerals Engineering* 24 (6):590–2. doi:10.1016/j.mineng.2011.02.014.
- Phengsaart, T., M. Ito, N. Hamaya, C. B. Tabelin, and N. Hiroyoshi. 2018. Improvement of jig efficiency by shape separation, and a novel method to estimate the separation efficiency of metal wires in crushed electronic wastes using bending behavior and “entanglement factor”. *Minerals Engineering* 129:54–62. doi:10.1016/j.mineng.2018.09.015.
- Pita, F., and A. Castilho. 2016. Influence of shape and size of the particles on jigging separation of plastics mixture. *Waste Management* 48:89–94. doi:10.1016/j.wasman.2015.10.034.
- Pita, F., and A. Castilho. 2017. Separation of plastics by froth flotation. The role of size, shape and density of the particles. *Waste Management* 60:91–9. doi:10.1016/j.wasman.2016.07.041.

- Pryor, E. J. 1965. *Mineral processing*. 3rd ed. London: Elsevier.
- Richard, G., S. Touhami, T. Zeghloul, and L. Dascalescu. 2017. Optimization of metals and plastics recovery from electric cable wastes using a plate-type electrostatic separator. *Waste Management* 60:112–22. doi:10.1016/j.wasman.2016.06.036.
- Richards, R. L., and S. B. Locke. 1940. *Textbook of ore dressing*. 3rd ed. New York, NY: McGraw-Hill.
- Singh, R. K., S. Dey, M. K. Mohanta, and A. Das. 2014. Enhancing the utilization potential of a low grade chromite ore through extensive physical separation. *Separation Science and Technology* 49 (12): 1937–45. doi:10.1080/01496395.2014.903495.
- Sivamohan, R. 1985. A study of gravity concentration with emphasis on surface phenomena. PhD diss., Lulea University of Technology.
- Thompson, J. V. 1958. The Humphreys spiral concentrator its place in ore dressing. *Mining Engineering* 84–7.
- Ulusoy, U. 2018. Dynamic image analysis of differently milled talc particles and comparison by various methods. *Particulate Science and Technology* 36 (3):332–9. doi:10.1080/02726351.2016.1248261.
- Ulusoy, U. 2020. Comparison of particle shapes of conventionally ground barite, calcite and talc minerals by dynamic imaging technique: A review. *EUREKA: Physics and Engineering* 5:80–90. doi:10.21303/2461-4262.2020.001406.
- Vision Analytical. 2021. Why particle shape is important. <https://particle-shape.com/why-particle-shape-is-important> (accessed October 8, 2021).
- Walsh, D. E., and E. G. Kelly. 1992. An investigation of the performance of a spiral using radioactive gold tracers. *Minerals and Metallurgical Processing* 9 (3):105–9. doi:10.1007/BF03402980.
- Wills, B. A., and J. Finch. 2015. Wills' mineral processing technology. In *An introduction to the practical aspects of ore treatment and mineral recovery*. 8th ed. Oxford: Butterworth-Heinemann.
- Zhao, Y., Y. Zhang, S. Bao, T. Liu, Y. Bian, X. Liu, and M. Jiang. 2013. Separation factor of shaking table for vanadium pre-concentration from stone coal. *Separation and Purification Technology* 115:92–9. doi:10.1016/j.seppur.2013.04.017.